Approaching the Ni percolation threshold by thin-film irradiation

1997 J. Phys.: Condens. Matter 9 2999

(http://iopscience.iop.org/0953-8984/9/14/014)

J. Phys.: Condens. Matter **9** (1997) 2999–3009. Printed in the UK PII: S0953-8984(97)74245-0

Approaching the Ni percolation threshold by thin-film irradiation

M Aprili† and P Nédellec

CSNSM, CNRS-IN2P3, Bâtiment 108, 91405 Orsay, France

Received 8 May 1996, in final form 30 December 1996

Abstract. We have reproduced a percolating structure in thin Ni films by an inhomogeneous sputtering process. The morphological disorder has been studied using TEM and '*in situ*' transport measurements during ion irradiation. The fluence dependence of the resistance shows a singularity following a 2D percolation law. The formation of the hole structure is consistent with a Poisson mechanism. A computer simulation developed using a code based on a Poisson statistics allows us to account for the experimental values of the percolation threshold ($p_c = 0.37$) and the overall shape of the infinite cluster.

1. Introduction

Electrical and optical properties of inhomogeneous films have been extensively studied ever since the initial work by Abeles *et al* appeared [1]. The correlation between the topology and the physical properties, like the electronic transport or the optical reflection, is of great interest as regards understanding the original physics related to non-Euclidean dimensionality. Two-dimensional inhomogeneous media have been studied mostly, because it is possible to image the actual sample topology by transmission electronic microscopy (TEM).

Such systems can be described as the mixing of two kinds of particle: conductive metallic grains and insulating holes, having typical sizes of 1–10 μm. When the concentration of the insulating part reaches a limit value, 'infinite' metallic paths are broken and the electrical connection is no longer established across the sample. Close to the percolation threshold p_c, effective-medium theories are no longer applicable, and the electrical conductivity is described by a critical law whose exponent depends on the dimensionality of the infinite cluster.

The purpose of this work is to study the percolation geometry of Ni samples obtained by inhomogeneous sputtering and their related electronic transport properties.

It is known that the energy deposited by heavy-ion irradiation is high enough to break bonds randomly within the target, and surface atoms can be sputtered [2]. Using the irradiation technique, we have been able to finely tune the characteristics of the inhomogeneous films produced, measuring their resistance at intervals between irradiation. We have also prepared films at given fluences, for the TEM studies. Quantitative analyses of the TEM images were performed using a specially developed code.

† Present address: University of Illinois at Urbana–Champaign, Urbana, IL 61801-3080, USA; e-mail: aprili@physics.uiuc.edu.

0953-8984/97/142999+11$19.50

We found that the ion beam mixing at the film–substrate interface changes the magnetic properties of Ni and modifies the crystal structure of the films. However, close to the percolation threshold p_c, the reduction of the metallic coverage rate dominates the electrical resistivity variation, which then follows a 2D percolation law. The formation of the holed structures is related to a statistical mechanism consistent with a Poisson process. Computer-simulated structures have been obtained which reproduce the general properties of the experimental ones.

2. Experimental method

The homogeneous films were prepared by evaporation under ultra-high vacuum (10^{-9} Torr). Our purpose was to carry out electrical measurements, before and after irradiation, as well as analysis by transition electron microscopy, on one and the same sample. To achieve this, we developed a special technique. We evaporated onto a glass substrate a layer of NaCl (1000 Å), a layer of SiO (250 Å), and finally, the sample. The sample was Ni film of about 150 Å thickness. After we had performed the resistivity measurements, the films were removed in water, deposited on a Cu grid, and analysed by transmission electron microscopy. The resistivity measurements showed that the effect of the NaCl substrate on the roughness of the sample is negligible.

Ni is a metallic ferromagnet, easy to grow as thin films. Beside the specific results presented here, we have also studied other scale-dependent phenomena, like electronic localization and the ferromagnetic transition, that are reported elsewhere [3, 4].

Homogeneous layers of nickel (thickness approximately 100 Å) were irradiated at room temperature with Xe at 150 keV using the CSNSM implanter [5]. The samples have a rectangular shape with a length L (8 mm) and a width l (1 mm): this geometry allowed homogeneous irradiation over the whole surface. We used a 150 keV xenon beam whose deposited energy, the mean energy transferred by the incident ions, is high (600 eV Å^{-1}); the sputtering yield for Ni is close to 10 (cf. TRIM simulations and published results [6]). RBS measurements show that the implanted Xe does not exceed 0.2%. After each irradiation dose ($\Phi = 10^{14}$–2×10^{14} ions cm^{-2}), resistance measurements of the film are taken. To study the structural modifications, at different irradiation stages, we produced samples of different resistances. These samples were then studied by electron microscopy. Previous studies had shown that the temperature has no effect on the formation of such holed systems [7].

We developed an image analysis program which allows TEM photograph analyses of irradiated films. After image scanning, the sample geometry, near the percolation threshold, is analysed stage by stage: digitization and thresholding of the metallic cluster, covering rate estimation, ascertaining of the infinite cluster, determination of the fractal dimensionality. Throughout this procedure, special care has been taken to avoid spurious effects: statistical treatments developed by Beghdadi and Le Negrate [8] have been used to choose the correct thresholding conditions; magnified TEM images as large as 20×30 cm have been scanned, resulting in a matrix of 800×600 digits [9].

3. Theory

Inhomogeneous metallic films have a disordered structure which can be studied using percolation theory [9, 10]. We consider a percolation model [11] whose critical laws could be extended to a continuous medium [12]. Near the percolation threshold p_c, the geometrical properties of the system depend on the observation scale. Two different behaviours appear

depending on the observation scale: on a large scale, the system is homogeneous; on a smaller scale, it has a fractal character. The correlation length ξ_p separates these two regimes. Approaching the threshold, ξ_p diverges, obeying a power law:

$$\xi_p = \xi_0(p - p_c)^{-\nu} \tag{1}$$

where ξ_0 is the distance between two nearest-neighbour sites, and p the percentage of occupied sites. The exponent, ν, depends on the dimensionality: $\nu = 4/3$ in 2D [13] and 0.88 in 3D [14].

In the fractal regime $L < \xi_p$, the number of sites comprising the infinite cluster depends on the measurement scale:

$$N_\infty(L) = \left(\frac{1}{\xi_0}\right)^{-\beta/\nu} L^{d-2-\beta/\nu}. \tag{2}$$

$\beta = 5/36$ in 2D and 0.4 in 3D. Therefore, the mass density, unlike that of a homogeneous system, also depends on the scale. The infinite cluster can then be considered as an object with a dimensionality $D = d - \beta/\nu$: this is the fractal dimensionality [15].

These results can be expanded to include electrical properties if one considers the sites to be connected by conducting links. When the system is of finite size, the conductance near the percolation threshold depends on the scale of measurement. In the fractal regime $L \ll \xi_p$, the sheet conductance varies according to a power law:

$$C_\square(L) = \sigma_0\left(\frac{1}{\xi_0}\right)^{-\beta/\nu} L^{d-\beta/\nu} \tag{3}$$

where σ_0 is the conductivity of each link. For lengths greater than ξ_p instead, the system is homogeneous, and the conductivity is independent of the scale, but depends on the percentage of occupied sites:

$$\sigma = \sigma_0(p - p_c)^\mu \tag{4}$$

where the geometrical factor $(p - p_c)^\mu$ accounts for the topology of the medium. For an inhomogeneous metallic film, the site occupation, p, must be replaced by the rate of metallic coverage which corresponds, for a network, to the occupied volume $x = fp$ (f is the filling factor). In fact, theoretical models [12] which describe the percolation problem in a continuous medium show that the critical exponents are universal, and independent of the particular form of the percolation structure studied; however, there is one exception with the 3D Swiss-cheese model which gives a value of the conductivity exponent μ larger than the lattice percolation one. In general, and especially for inhomogeneous films, the scale ξ_p is very much smaller than the scale used for electrical measurements of the sample. The conductivity is therefore described by relation (4).

4. Results

Figure 1(a) shows the sheet resistance as a function of the irradiation fluence. Two different behaviours occur as a function of the dose Φ. For weak doses $\Phi < 4 \times 10^{15}$ ions cm^{-2} the resistance varies slowly; for high doses $\Phi > 4 \times 10^{15}$ ions cm^{-2} the variation increases and the resistance diverges.

Using TEM analysis, we can correlate these two regimes with the modifications of the film topology. In figure 1(b) we report a TEM image of a high-dose-irradiated film, the dark regions being the conducting channels and the white ones the substrate.

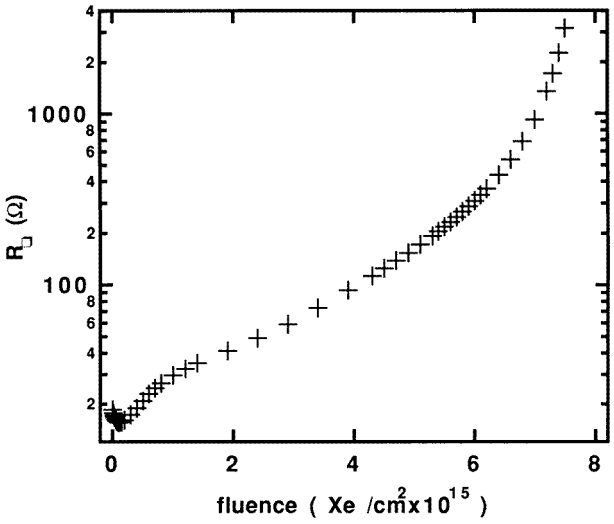

(a)

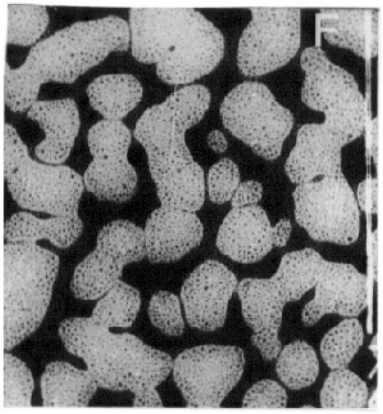

(b)

Figure 1. (a) The resistance per square of an irradiated Ni film as a function of dose. (b) An inhomogeneous structure is built up in the irradiated Ni film. The dose is 7.4×10^{15} ions cm^{-2}.

4.1. The homogeneous regime

For doses lower than 4×10^{15} ions cm^{-2}, irradiation produces several effects: an increase of the crystal sizes, a thinning of the film, and the creation of atomic disorder. Because of these effects, the resistance depends on the dose. The annihilation of the grain boundaries produces a decrease of the bulk resistivity, which is experimentally observed for a low radiation dose, $\Phi < 2 \times 10^{14}$ ions cm^{-2}. However, this effect is rapidly saturated; starting from 3×10^{14} ions cm^{-2} the granular structure is no longer modified by the irradiation as observed by TEM [4]. The resistance variation for higher doses is related only to the reduction of the film thickness and to the atomic disorder.

The RBS study shows that there is a thickness reduction only in the homogeneous regime [16]; for $\Phi > 4 \times 10^{15}$ ions cm^{-2} the thickness is constant. This result is coherent

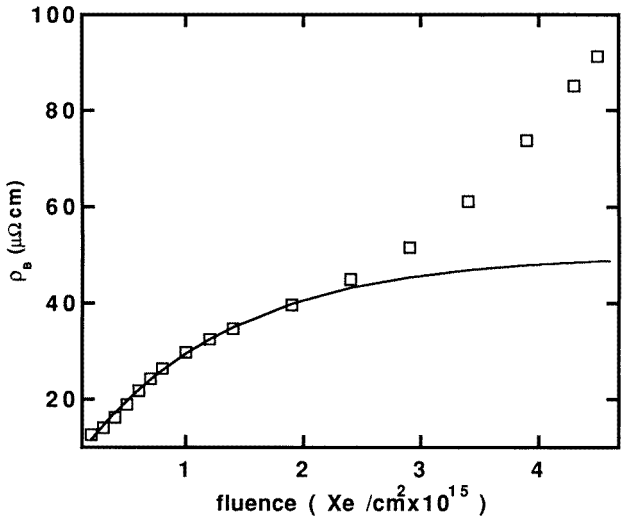

(a)

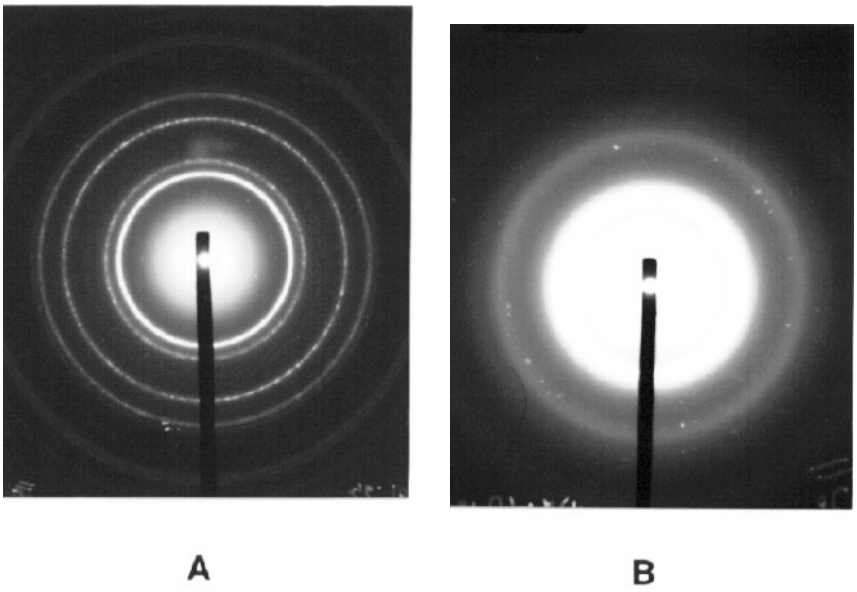

(b)

Figure 2. (a) The bulk resistivity ρ_B as a function of the irradiation dose. (b) TEM diffraction patterns for two irradiation doses: A: 2.6×10^{15} ions cm^{-2}; B: 4.4×10^{15} ions cm^{-2}.

with the ones obtained by means of the Hall measurements. The sputtering coefficient is estimated to be $Y \approx 10$, in good agreement with the values found in the literature [6].

The amount of atomic disorder increases during the irradiation of the sample. If we assume that the product $\rho_B l_B$ is independent of the irradiation level (l_B is the bulk mean free path), Fuchs's law allows us to deduce the variation of the bulk resistivity ρ_B which is presented in figure 2(a) ($\rho_B(300\ \mathrm{K}) = 17\ \mu\Omega$ cm and $l_B = 220$ Å).

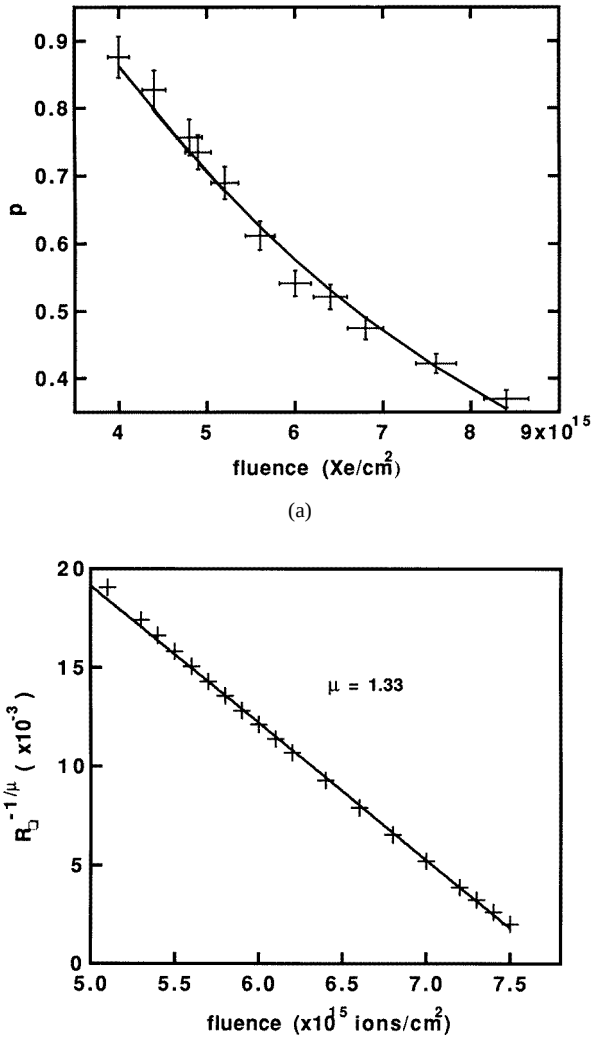

Figure 3. (a) The covering rate as a function of the irradiation dose. The solid line is calculated using a Poisson-type statistical mechanism for the hole formation (see the text). (b) The critical behaviour of the resistance as a function of the irradiation dose close to the percolation threshold.

The variation of ρ_B for $\Phi < 2 \times 10^{15}$ ions cm^{-2} is well known [17] and is due to the creation and saturation of atomic defects. We consider the relation

$$\rho_B = \rho_0 + \rho_s\{1 - \exp(-\gamma\Phi)\} \tag{5}$$

which describes the variation of ρ_B on the basis of the hypothesis that the probability of creation of an atomic defect, during the irradiation, is proportional to the difference between the saturation value ρ_s and the resistivity $\rho_B(\Phi)$. The parameter γ behaves as the effective cross section for the creation of atomic defects. The best agreement between the theoretical relation and the experimental measurements (the full line in figure 2) is obtained for $\rho_s = 45\ \mu\Omega$ cm and $\gamma = 0.78 \times 10^{15}$ cm^2/ion. For $\Phi > 2.6 \times 10^{15}$ ions cm^{-2} the

experimental behaviour diverges considerably from the theoretical one described by relation (5). Why is this?

4.2. Amorphization

We characterize the structural behaviour of the irradiated samples by electronic diffraction. The diffraction patterns for two different irradiation stages are shown in figure 2(b). We observe, between the patterns A ($\Phi = 2.6 \times 10^{15}$ ions cm^{-2}) and B ($\Phi = 4.4 \times 10^{15}$ ions cm^{-2}), a change of the initial polycrystalline structure, going towards an amorphized structure. It is known [18] that, like other pure metals (except Ga and Bi), Ni does not amorphize with the increase in disorder on the atomic scale. The amorphous state is stabilized by the introduction of covalent impurities, such as Si or O, which allow partial reorientation of atomic bonds.

We estimate that the amorphous state is due to ion beam mixing at the Ni/SiO interface, the deposition energy being very high (about 600 eV Å^{-1}). Using the model developed by Desimoni and Traverse [19] and assuming that Ni and Si are the only mixed species, we can estimate the size δ of the mixing region:

$$\delta^2 = \frac{0.035}{\rho^2}\frac{F_d^2\Phi}{\Delta H_{coh}}\left(1 + 27.4\frac{\Delta H_{mix}}{\Delta H_{coh}}\right) \tag{6}$$

where ρ is volumic mass of the compound which is forming, ΔH_{coh} the average of the two cohesion energies, and ΔH_{mix} is the mixing enthalpy. An underestimate of δ may be obtained by taking the leading term in the above expression. Using ΔH_{coh} and the volumic mass of pure Ni, we get a rough estimate of δ: the mixing zone for a dose of 5×10^{15} ions cm^{-2} is of the order of 100 Å—that is, almost the initial film thickness. This effect explains the rapid variation of ρ_B for $\Phi > 2.6 \times 10^{15}$ ions cm^{-2} (figure 2). From the experimental behaviour $\rho_B(\Phi)$ we can determine the variation $\Delta\rho/\Delta\Phi$. We obtain $\Delta\rho/\Delta\Phi = 2.74 \times 10^{-20}$ Ω cm^3/ion. Assuming that the composition is $Ni_{1-x}Si_x$, the amorphous state is attained at a Si concentration of around 15% [20]. It is therefore possible to evaluate the ratio $\Delta\rho/\Delta c$, where $\Delta\rho/\Delta c = (\Delta\rho/\Delta\Phi)(\Delta\Phi/\Delta c)$. We find $\Delta\rho/\Delta c = 8$ μΩ cm/at.%.

4.3. The inhomogeneous regime

We have shown that for $\Phi > 4 \times 10^{15}$ ions cm^{-2} the morphology of the film is modified and an inhomogeneous structure is produced. With the help of the computer code that we have developed, we can study the geometrical properties of the irradiated samples and analyse their effects on the electrical properties.

We determine, to start with, the variation in the coverage rate p as a function of the irradiation dose, considering only the samples characterized by continuous metallic paths: see figure 3(a). We estimate the percolation threshold to be $p_c = 0.37$ from our experiments.

Let us assume that the hole formation mechanism is purely statistical. Assuming that hole creation by an incident ion impact is a rare event, the coverage rate is described by a Poisson process:

$$p = \exp[-\gamma_t(\Phi - \Phi_0)] \tag{7}$$

where γ_t is the effective cross section for hole formation, and Φ_0 being the dose for which the first holes appear. Relation (7) is presented in figure 3(a). We have determined that $\gamma_t = 2 \times 10^{-16}$ cm^2 and $\Phi_0 = 3.4 \times 10^{15}$ ions cm^{-2}. In the dose interval $\Delta\Phi$, near the threshold, the experimental results of figure 3(a) are well described by the development,

to the first order, of the function (7). There is, therefore, a linear relationship between the dose and the covering rate.

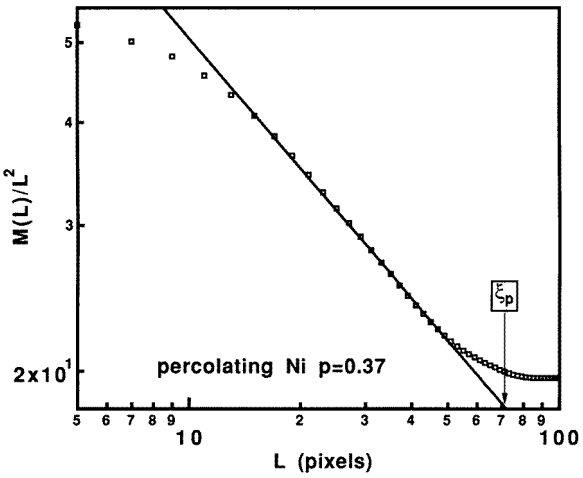

Figure 4. A log–log plot of the mass density of the infinite cluster as a function of the scale (the typical grain size is $L = 10$).

This result allows the analysis of the irradiation curve (figure 1(a)) in terms of a decrease of the metallic coverage rate. In a percolation system, the conductivity varies as a function of $p - p_c$ according to expression (4). If p is proportional to Φ, we expect the resistance to obey a power law as well, characterized by the same critical exponent:

$$R = \frac{R_0}{(\Phi_c - \Phi)^{\mu}}. \tag{8}$$

The critical behaviour is shown in figure 3(b), where the representation of $R^{-1/\mu}$ as a function of Φ allows the determination of μ independently of the knowledge of the value of the critical dose Φ_c. We obtain a linear relation for $\mu = 1.33$, in very good agreement with the two-dimensional theoretical value, $\mu = 1.3$. This result is consistent with a small variation in the critical regime of the coefficient R_0, characterizing the resistance at the conducting channel scale. Therefore in this regime, the thicknesses and the resistivities of the films seem to be constant. From $R_0 = 2.08 \times 10^{-18}$ Ω cm^2/ion, we can estimate the saturation value of the bulk resistivity: we find 117 $\mu\Omega$ cm which is in agreement with the estimated value for the amorphous homogeneous films.

The critical dose is obtained by extrapolation to $R^{-1/\mu} = 0$. It is found that $\Phi_c = 7.8 \times 10^{15}$ ions cm^{-2}, which is only around 10% less than the value obtained by image analysis. The difference corresponds to a layer thinning by approximately 6 Å. Because of the mixing effects, an insulating layer of this thickness could easily form at the Ni/SiO interface. If the thickness of the insulating layer is less than the average thickness of the film, this effect does not change the critical exponent μ.

Let us focus on the geometrical properties of the percolating structure that we realized. Approaching the percolation threshold, the resistivity shows a critical behaviour, described by a percolation law in 2D (see expression (4)). However, on a small scale $L < \xi_p$, the fractal behaviour modifies the electrical transport laws of the homogeneous systems. Let us analyse the fractal dimensionality of the percolating structure obtained.

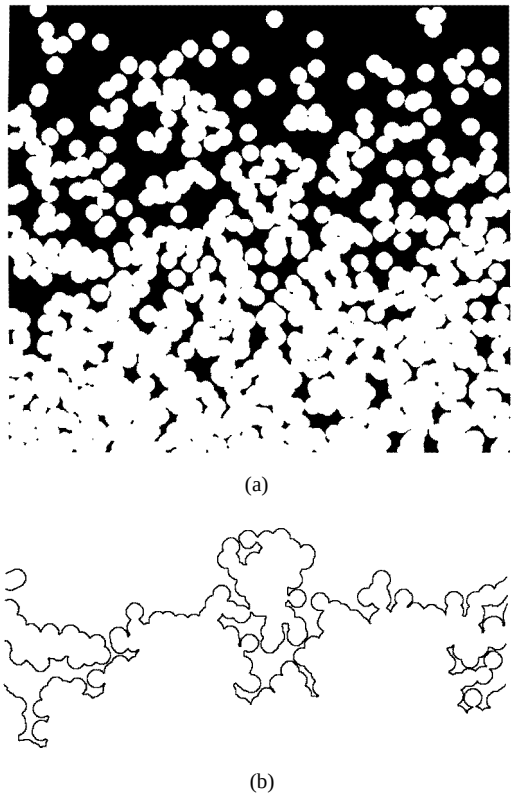

(a)

(b)

Figure 5. (a) A computed image of a hole distribution according to a concentration gradient. (b) The frontier between connected holes and connected metal.

The mass density $m(L)$ of the infinite cluster depends on the measurement scale. We measure $m(L)$ inside a square of side length L, for different values of L. We ascertain the variation of $m(L)$ as a function of square size. The result is presented in figure 4. For sizes greater than the metallic grain size (200 Å) and less than 600 Å, the density of the infinite cluster varies as a function of the scale L. The variation of δ can be analysed using the scaling law which describes the behaviour of the mass density in a fractal system. The density of the medium is non-Euclidean and we find that $D = 1.55 + 0.05$. The theoretical value for the fractal dimensionality calculated using the model of the percolation network is $D = 1.89$. It is known [21] that the limited range of sizes L used to measure D (as is always the case in a real system) leads to its value being underestimated. Moreover, accurate thresholding is difficult to achieve for low-contrast TEM pictures. This also gives a low value for the experimental D, as we will show using a suitable model. At larger scales, the density remains constant and the sample appears homogeneous. The correlation length defines the limit between the two regimes; here it is about 600 Å, i.e. 5–6 grain diameters.

Let us now consider the following percolation model. Holes are randomly punched on a surface, based on a Poisson process observed in the percolating structure formation. One can determine accurately the percolation threshold and the critical exponent of the correlation length without performing a full statistical analysis [21, 22], by using the gradient method. A single image is computer generated using a given gradient in the hole concentration from

the top to the bottom of the picture (figure 5(a)). It is worth noticing that this picture is not a simulation of one typical sample, but a tool for evaluating the properties of this percolation model. One can compute the number of holes in each line using the exponential law (see expression (7)), where γ_t is the normalized area of a single hole, and Φ the number of holes.

The frontier of the metallic cluster is defined as the external envelope of the connected black sites (figure 5(b)). The frontier of the holes is symmetrically computed. These lines are in the region where the covering rate is close to p_c; we can therefore determine them. Two important results have been obtained from these simulations. We can calculate the percolation threshold as the average distribution of holes on the border line; a value of $p_c = 0.38$ is found, close to the experimental one. Moreover, the fractal dimensionality of the frontier is found to be $D_f = 1.61$, lower than the expected one for a lattice ($D_f = 7/4$). In fact, Rosso [22] has shown that this exponent rapidly decreases when the size of the punched holes increases. Such a sensitivity of the shape of the border line to the hole size makes the experimental determination of the fractal dimensionality of the infinite cluster delicate. A slightly inaccurate thresholding may strongly modify the shape of the frontier, and therefore leads to D being underestimated in this situation.

5. Conclusions

By irradiation of Ni thin films (100 Å) with heavy ions, we have produced disorder on two specific scales: an atomic scale (a few Å), and a macroscopic scale (1000 Å). The electrical measurements together with the TEM image analysis display three regimes, as a function of the ion dose.

(1) The homogeneous regime: $\Phi < 2.6 \times 10^{15}$ ions cm^{-2}. The film is homogeneous and the resistance variation is due to an increasing atomic disorder and a decreasing thickness.

(2) The medium regime: 2.6×10^{15} ions cm^{-2} $< \Phi < 4.4 \times 10^{15}$ ions cm^{-2}. The polycrystalline structure of the film is modified. Ionic mixing causes an amorphization of the sample.

(3) The inhomogeneous regime: $\Phi > 4.4 \times 10^{15}$ ions cm^{-2}. The morphology of the film is affected and a holed system is created by sputtering. The metallic covering rate as a function of dose follows a Poisson law, and the percolation transition is reached for $p_c = 0.37$. Close to the threshold, the electrical conductivity is described by a power law, whose critical exponent $\mu = 1.33$ is typical of a 2D behaviour. The fractal dimensionality of the infinite cluster analysed by the scaling law of the mass density gives $D = 1.6$. This is not the expected value for a standard percolation model ($D = 1.89$); however, arguments have been given to explain the actual value using the hole concentration gradient percolation model computed by a Poisson process. Moreover, the theoretical threshold for this model is $p_c = 0.38$, very close to the experimental one: $p_c = 0.37$.

Acknowledgments

The authors are obliged to Marie-Odile Ruault for the TEM analysis and to Judith Desimoni and Agnès Traverse for many stimulating discussions about the ion irradiation effects. It is a pleasure to acknowledge Harry Bernas and Jerôme Lesueur for a critical reading of the original manuscript.

References

[1] Abeles B, Sheng P, Coutts M D and Arie Y 1975 *Adv. Phys.* **24** 407
[2] Papandreou N and Nédellec P 1992 *J. Physique* I **2** 707
[3] Aprili M, Nédellec P and Dumoulin L 1996 *Solid State Commun.* **93** 221
[4] Aprili M, Lesueur J, Dumoulin L and Nédellec P 1997 *Solid State Commun.* **102** 41
[5] Cottereau E, Camplan J, Chaumont J, Meunier R and Bernas H 1990 *Nucl. Instrum. Methods* B **45** 293
[6] Andersen H H and Bay H L 1981 *Sputtering by Particle Bombardment 1 (Springer Topics in Applied Physics 47)* ed R Behrisch (Berlin: Springer) p 175
[7] Papandreou N 1989 *Thesis* Université Paris Sud
[8] Beghdadi A and Le Negrate A 1989 *Comput. Vision* **46** 162
[9] Kapitulnik A and Deutscher G 1982 *Phys. Rev. Lett.* **49** 1444
[10] Octavio M, Gutierrez G and Aponte J 1987 *Phys. Rev.* B **36** 2461
Koch R H, Laibowitz R B, Allessandrini E I and Vigiano J M 1985 *Phys. Rev.* B **32** 6932
[11] Stauffer D and Aharony A 1992 *Introduction to Percolation Theory* (London: Taylor and Francis)
[12] Halperin B I, Feng S and Sen P N 1985 *Phys. Rev. Lett.* **54** 2391
See also
Feng S, Halperin B I and Sen P N 1987 *Phys. Rev.* B **35** 197
[13] den Nijs M P M 1979 *J. Phys. A: Math. Gen.* **12** 1857
[14] Strenski P N, Bradley R M and Debierre J M 1991 *Phys. Rev. Lett.* **66** 133
[15] Gefen Y, Aharony A, Mandelbrot B and Kirkpartrick S 1991 *Phys. Rev. Lett.* **47** 1771
[16] Aprili M 1994 *Thesis* Université Paris Sud
[17] Averbach R S, Benedek R and Merkle K L 1978 *Phys. Rev.* B **18** 4156
[18] See the discussion in
Cohen C, Benyagoub A, Bernas H, Chaumont J, Thomé L, Berti M and Drigo A V 1985 *Phys. Rev.* B **31** 5
[19] Desimoni J and Traverse A 1993 *Nucl. Instrum. Methods* B **80/81** 91
[20] Durand J 1983 *Glassy Metals II (Springer Topics in Applied Physics 53)* ed H J Güntherodt and H Beck (Berlin: Springer)
[21] Rosso M, Gouyet J F and Sapoval B 1985 *Phys. Rev.* B **32** 6053
[22] Rosso M 1989 *J. Phys. A: Math. Gen.* **22** L131